Tuning in magnetic modes in $Tb(Co_xNi_{1-x})_2B_2C$: From longitudinal spin-density waves to simple ferromagnetism

M. ElMassalami,[1] H. Takeya,[2] B. Ouladdiaf,[3] R. Maia Filho,[1] A. M. Gomes,[1] T. Paiva,[1] and R. R. dos Santos[1]

[1]*Instituto de Fisica, Universidade Federal do Rio de Janeiro, Caixa Postal 68528, 21945-970 Rio de Janeiro, Brazil*

[2]*National Institute for Materials Science, 1-2-1 Sengen, Tsukuba, Ibaraki 305-0047, Japan*

[3]*Institut Laue-Langevin, B.P. 156, F-38042 Grenoble Cedex 9, France*

(Received 28 February 2012; published 9 May 2012)

Neutron diffraction and thermodynamic techniques were used to probe the evolution of the magnetic properties of $Tb(Co_xNi_{1-x})_2B_2C$. A succession of magnetic modes was observed as x is varied: the longitudinal modulated $\vec{k} = (0.55,0,0)$ state at $x = 0$ is transformed into a collinear $\vec{k} = (1/2,0,1/2)$ antiferromagnetic state at $x = 0.2$, 0.4 then into a transverse c-axis modulated $\vec{k} = (0,0,1/3)$ mode at $x = 0.6$, and finally into a simple ferromagnetic structure at $x = 0.8$ and 1. Concomitantly, the low-temperature orthorhombic distortion of the tetragonal unit cell at $x = 0$ is reduced smoothly such that for $x \geqslant 0.4$ only a tetragonal unit cell is manifested. Though predicted theoretically earlier, this is the first observation of the $\vec{k} = (0,0,1/3)$ mode in borocarbides; our findings of a succession of magnetic modes upon increasing x also find support from a recently proposed theoretical model. The implication of these findings and their interpretation on the magnetic structure of the RM_2B_2 C series are also discussed.

DOI: 10.1103/PhysRevB.85.174412 PACS number(s): 75.50.Cc, 71.27.+a

Rare-earth $4f$ moments at regular crystalline sites of intermetallic matrices are subjected to a variety of competing interactions, such as the Ruderman-Kittel-Kasuya-Yosida (RKKY), crystalline electric field, magnetoelastic, and dipolar interactions.[1,2] A particular class of such $4f$ intermetallics is the quaternary isomorphous borocarbides RM_2B_2C (R is a rare earth or Y, and M is a transition metal), which have been found to exhibit coexistence between superconductivity and magnetism for a judicious choice of R and M.[3–8] Apart from the interesting issue of coexistence (which highlights the importance of electron interactions, with themselves as well as with the $4f$ moments), the magnetic properties of these materials pose a challenging problem in their own right, especially when R is magnetic and M is nonmagnetic. For the interesting case of $M =$ Co or Ni, Table I indicates that, for fixed R, the Co-based members exhibit collinear and equal-amplitude ferromagnetic (FM)/antiferromagnetic (AFM) structures;[9–11] by contrast, the Ni-based members exhibit a variety of modulated structures, few equal-amplitude and commensurate AFM structures, and an absence of FM modes.[12]

Rhee *et al.*[13] have calculated the generalized susceptibility for borocarbides from band structures obtained through the local-density approximation (LDA): for a fixed pair R and M, three incommensurate peaks were predicted near $\vec{k}_1 = (0.6,0,0)$, $\vec{k}_2 = (0,0,0.9)$, and $\vec{k}_3 = (0,0,0.3)$. Though calculated for the nonmagnetic $LuNi_2B_2C$, the results were expected to be valid for all R, with the precise position and sharpness of each peak depending on R and M. Experimentally, both $\vec{k}_1$ and $\vec{k}_2$ modes show up in $HoNi_2B_2C$ and, moreover, $\vec{k}_1$ is evident in, for example, $R =$ Er, Tb, Gd (Ref. 12), but so far $\vec{k}_3$ has not been observed in borocarbides. It is recalled that this model does not account for many modes [e.g. (0,0,1), (1/2,0,1/2) in RNi_2B_2C and (1/2,0,1/2), (0,0,0) RCo_2B_2C]; in Ref. 13, the authors attributed this to the fact that their theory does not contemplate any mechanism leading to an interplay between magnetism and superconductivity. Then a complementary theoretical approach contemplating both magnetism and superconductivity, and from which their interplay can be investigated, would be highly desirable. Bertussi *et al.*[14] proposed such a model from which a succession of magnetic modes exist even in the absence of superconductivity; see below.

This very particular case of the surge of various magnetic modes even in the absence of superconductivity can best be tested in the $Tb(Co_x\ Ni_{1-x})_2B_2C$ series wherein both end members are nonsuperconducting. With this in mind, here we report on the mapping out of the magnetic modes of $Tb(Co_xNi_{1-x})_2B_2C$ solid solutions. In view of the markedly distinct magnetic structures of the Ni and Co-based compounds, it is certainly of interest to investigate in detail how the magnetic (e.g., modes and moments) and structural properties develop as M is changed (almost) continuously between these two limits. The choice of this particular $R =$ Tb was dictated by the following features: (i) the higher transition temperatures of the end members (in comparison with the other pairs appearing in Table I) allows for an investigation over a wide temperature range and (ii) the incomensurate linear spin density wave (LSDW) mode of $TbNi_2B_2C$ is transformed into a commensurate FM state of $TbCo_2B_2C$, thus allowing, in principle, for several $\vec{k}$ vectors setting in. We will then be particularly interested in elucidating whether this M-induced mode transformation is abrupt, or if there are additional intermediate modes, in which case the determination of how the $\vec{k}$ vectors are modified upon varying M should highlight the mechanisms at play. For completeness, we should mention that several studies of the magnetic and electronic properties of $R(Co_xNi_{1-x})_2B_2C$ have been reported earlier (see, e.g., Refs. 5 and 8 and references therein).

Polycrystalline samples of $Tb(Co_xNi_{1-x})_2B_2C$ ($x =$ 0,0.2, ...,1) with 99.5% ^{11}B-enriched were prepared by the conventional arc-melt method; all samples were annealed for 20 hours at 1100 °C. Room-temperature conventional x-ray diffraction analysis of polycrystalline samples (not shown) indicated a single phase character for all compositions; the

TABLE I. Magnetic structures and transition temperatures, T_{cr}, of the isomorphous RM_2B_2C (R = Tm, Er, Ho, Dy, Tb; M = Ni, Co) series. TSDW (LSDW) denotes a transverse (longitudinal) modulated spin-density wave, $\vec{k}$ is the propagation wave vector, while $\vec{\mu}$ is the moment polarized along the easy axis. The magnetic properties of RNi_2B_2C were taken from Refs. 12 and 15, while those of RCo_2B_2C were taken from Refs. 9–11.

R	Tm		Er		Ho		Dy		**Tb**	
M	Co	Ni	Co	Ni	Co	Ni	Co	Ni	**Co**	**Ni**
T_{cr} (K)	0.8	1.53	4.0	6.8	5.4	5.0	8.0	10.6	**6.3**	**15.0**
structure	FM	TSDW	AFM	TSDW	FM	AFM	FM	AFM	**FM**	**LSDW**
$\vec{k}$	(0,0,0)	(0.093,0.093,0)	(1/2,0,1/2)	(0.553,0,0)	(0,0,0)	(0,0,1)	(0,0,0)	(0,0,1)	**(0,0,0)**	**(0.555,0,0)**
$\lvert\vec{\mu}\rvert$ (μ_B)	∼1	3.8	6.8(2)	7.2	7.2(2)	8.6	>5.2(2)	8.5	**7.6**	**7.8**
orientation	$\vec{c}$	$\vec{c}$	$\vec{b}$	$\vec{b}$	$\vec{a}+\vec{b}$	$\vec{a}+\vec{b}$	$\vec{a}+\vec{b}$	$\vec{a}+\vec{b}$	$\vec{a}$	$\vec{a}$

lattice parameters, as obtained from the Rietveld analysis,[16] are in excellent agreement with the reported values.[10,12,17,18] Powder neutron-diffractograms were collected at the high resolution powder diffractometer D2B of the Institut Laue-Langevin (ILL), France ($\lambda = 1.6$ Å, $T = 1.5$ and 30 K), and were analyzed by the same Rietveld package. The diffractograms of the end members were not measured since these have already been determined.[10,12,19] Magnetizations and susceptibilities (2 K $< T <$ 20 K and $H \leqslant 90$ kOe) were measured on a Physical Properties Measurement System of Quantum Design; specific heat curves (1.8 K $< T <$ 40 K and $H = 0$, 30 kOe) were measured on a relaxation-type calorimeter using the same environment as that used for the magnetization measurements. The results obtained from these thermodynamic techniques (which will appear elsewhere[20]) provide independent confirmation of the picture to be discussed below.

The 30 K nuclear diffractograms [Figs. 1(a)–1(d)] exhibit single-phase tetragonal structures ($I4/mmm$) with Tb, Co_xNi_{1-x}, B, and C being at $2a$, $4d$, $4e$, and $2b$ sites, respectively.[12,17] On the other hand, data at 1.5 K, Figs. 1(e)–1(h), reveal a superposition of magnetic and nuclear subpatterns. Because of the well-known orthorhombic distortion of $TbNi_2B_2C$ (Refs. 18, 21, and 22), no subtraction of the 30 K nuclear contribution was attempted for the Ni-rich samples; rather, for the $x < 0.4$ compositions, the 1.5 K nuclear subpatterns were analyzed assuming a tetragonal-to-orthorhombic distorted unit cell [see inset of Fig. 1(e)]. Applying this same analysis to the low-temperature $x \geqslant 0.4$ diffractograms yielded $a \approx b$; it is then clear that, for all $x \geqslant 0.4$, no structural distortion takes place. Accordingly, for these nuclear diffractograms, the above-mentioned $I4/mmm$ space group was used. The whole-pattern fits are shown in Figs. 1(e)–1(h), and the (most important) fit parameters are shown in Table II and Figs. 2(b)–2(d).

The magnetic structures of Table II are visualized in Fig. 3. The moment orientation for each composition was taken to be along the a axis of the nuclear unit cell based on the reported features of the parent TbM_2B_2C compounds.[18,19,21,22] The incommensurate structure of the pure Ni sample ($x = 0$) becomes, for $x = 0.2$ and 0.4, a collinear AFM mode with $\vec{k}$ =(1/2,0,1/2) (i.e., AFM along the a and c axes and FM along the b axis); this structure is different from the a-axis modulated mode of $TbNi_2B_2C$, but similar to that of $ErCo_2B_2C$ (Ref. 9), and $NdNi_2B_2C$ (Ref. 12). One should note that while the magnetic moment for $x = 0.2$ is $|\vec{\mu}| = 7.6\,\mu_B$ (thus very close to that for $TbNi_2B_2C$), for $x = 0.4$ it is $|\vec{\mu}| = 3.7(2)\,\mu_B$ which is, surprisingly, less than half of the expected value. Such anomalous behavior is also evident in the thermodynamical properties.[20] In the opposite limit of the Co-rich region, the $x = 0.8$ sample displays a commensurate $\vec{k} = (0,0,0)$ mode, just as for $TbCo_2B_2C$ (Ref. 10); it should be noted that $|\vec{\mu}(x = 0.8)| = 8.7(2)\,\mu_B$, which is 14% larger than $|\vec{\mu}(x = 1)| = 7.6\,\mu_B$.

The magnetic structure for $x = 0.6$ is a transverse c-axis–modulated spin-density wave with $\vec{k} = (0,0,0.33 \pm 0.01) \approx (0,0,1/3)$: the FM planes are modulated, rotated, and stacked along the c axis with a period three times longer than that of the nuclear cell and with an amplitude of $10.8\,\mu_B$. At lower temperatures, this mode will be squared-up due to the surge of higher, odd Fourier harmonics;[12] then, the moment of this squared-up SDW will be, according to Fourier analysis, $(\pi/4) \cdot 10.8\,\mu_B = 8.5\,\mu_B$, in good agreement with the moment found for the neighboring $x = 0.8$ composition.

It should be noticed that the strength of the magnetic moment evolves nonmonotonically with x, with the lowest value

TABLE II. Magnetic properties of $Tb(Co_xNi_{1-x})_2B_2C$. μ_{ND} is the zero-field moment as obtained from neutron diffraction analysis, while μ_M is the moment at 90 kOe as obtained from magnetization isotherms at 2 K. Data for $x = 0$ and $x = 1$ were taken from Refs. 12 and 10, respectively.

x	0	0.2	0.4	0.6	0.8	1.0
T_{cr} (K)	15.0(2)	12.0(2)	8.3(3)	8.8(3)	7.4(2)	6.6(2)
structure	LSDW	AFM	AFM	TSDW	FM	FM
$\vec{k}$	(0.55,0,0)	(1/2,0,1/2)	(1/2,0,1/2)	(0,0,1/3)	(0,0,0)	(0,0,0)
$\lvert\vec{\mu}\rvert_{ND}$ (μ_B)	7.8	7.6(1)	3.7(2)	8.5(2)	8.7(2)	7.6
$\lvert\vec{\mu}\rvert_{M(90\,kOe)}$ (μ_B)	7.4(1)	4.1(1)	7.6(2)	7.7(1)	7.6(1)	7.2
easy axis	$\vec{a}$	$\vec{a}$	$\vec{a}$	$\vec{a}$	$\vec{a}$	$\vec{a}$

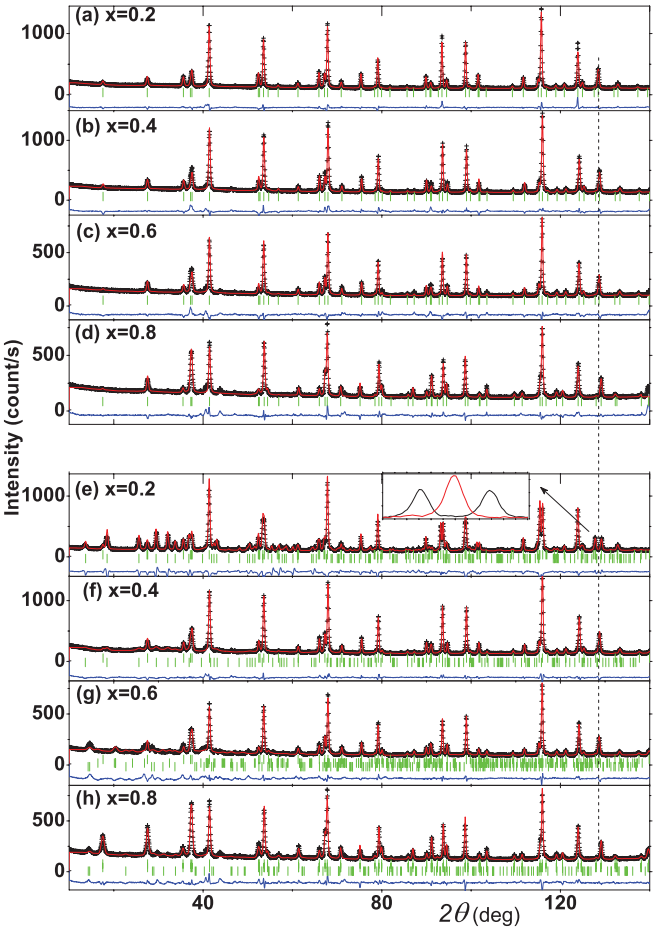

FIG. 1. (Color online) Neutron diffractograms of $Tb(Ni_xCo_{1-x})_2B_2C$, measured at (a)–(d) $T = 30$ K and (e)–(h) at $T = 1.5$ K. *Symbols:* measured intensities; *vertical short bars:* Bragg positions of the nuclear and magnetic peaks; *solid line:* Rietveld refined fit. The vertical dashed line highlights the orthorhombic splitting of the tetragonal (3,0,5) peak into the pairs (3,0,5), (0,3,5). Inset: an expansion showing, for $x = 0.2$, the single peak at 30 K (thin line) is orthrohmbic-split at 1.5 K into two peaks (thick line). Space groups, positions, and occupations are given in text; thermal parameters are the same as those reported by Lynn *et al.* (Ref. 12). $\vec{k}$ and $\vec{\mu}$ are given in Table II, while the lattice parameters are shown in Fig. 2. The R factors are in the range of 3–10.

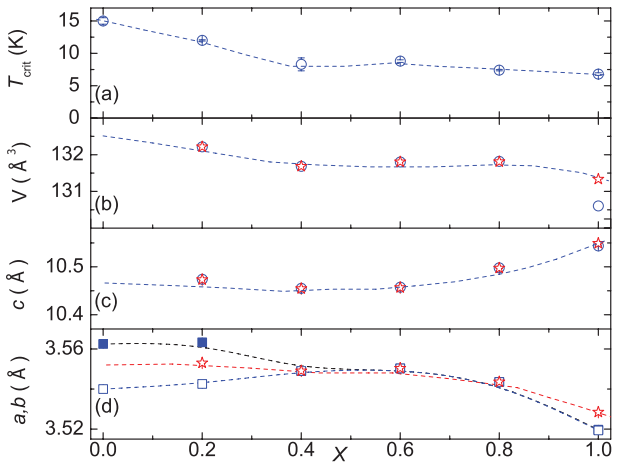

FIG. 2. (Color online) (a) The dependence with the Co fraction x of the magnetic critical temperature T_{cr} and of the lattice parameters: (b) unit cell volume V, (c) lattice constants c, and (d) a,b. In panels (b)–(d), stars and squares correspond, respectively, to fits to tetragonal (30 K) and orthorhombic (1.5 K) unit cells; in panel (d), filled and open symbols represent the a and b lattice constants. Dashed lines are guides to the eye. Data for $x = 0$ were taken from Refs. 18,21, and 22 while those for $x = 1$ were taken from Ref. 10.

being found within the neighborhood of $x = 0.4$. Furthermore, the observed propagation vectors $\vec{k} = (0.55,0,0)$, $(1/2,0,1/2)$, $(0,0,1/3)$, and $(0,0,0)$ form a subgroup of the main magnetic group, which for borocarbides was predicted based on rigorous symmetry analyses of representation theory.[23] Evidently, among this multitude of $\vec{k}$ modes, the $\vec{k} = (0,0,1/3)$ mode is unique since it has not been encountered in previous studies of either RCo_2B_2C (Refs. 9–11) or RNi_2B_2C (Ref. 12), though it is not forbidden by representation theory.[23]

Our findings agree with the results from available theoretical approaches. First, as mentioned before, the LDA calculations of Ref. 13 predict three possible magnetic modes in borocarbides, one of which, $\vec{k}_3$, has only been observed in the present system. Second, a simple analysis suggests that the surge of a succession of magnetic modes reported here may be attributed to a competition between opposing tendencies of magnetic couplings. Indeed, the oscillatory RKKY interaction between the local moments is mediated by the conduction electrons, so that its spatial scale of oscillation is set by the Fermi momentum k_F; then, due to electron count, k_F would be different in the Co-pure system and in the Ni-pure

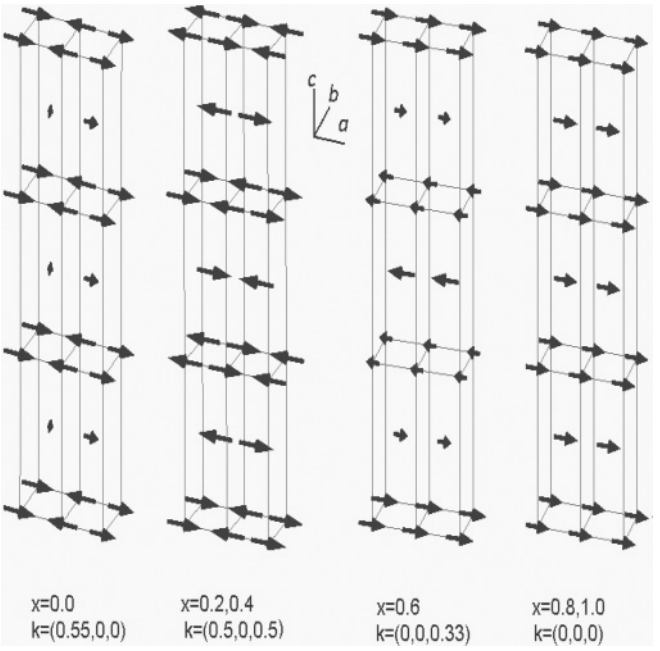

FIG. 3. The magnetic structures of $Tb(Co_xNi_{1-x})_2B_2C$. Neither the moment strength nor the unit-cell dimensions were drawn to scale. Following Table II, the Tb moments were taken to be polarized along the $\vec{a}$ axis.

isomorph. Assuming a continuously varying effective k_F upon "continuous" substitution of Ni by Co, the associated variation in the RKKY coupling transforms the AFM mode at the Ni-based limit into the FM mode at the Co-based limit through a succession of intermediate modes.

Though this scenario is qualitatively consistent with our observations, a step beyond this simplified picture is to contemplate superconductivity and its coexistence with magnetism, which in the context of the borocarbides is crucial to reach a unified description. As mentioned in the Introduction this task has been undertaken by Bertussi *et al.*[14] who proposed an *effective* microscopic model in which the conduction electrons are subject to a pairing interaction, say an attractive Hubbard-U term, while they also mediate the magnetic interaction between local moments via a Kondo-like coupling J. The phase diagram obtained predicts a multitude of magnetic modes setting in as $|J|$ increases, which can coexist (or not) with superconductivity, depending on the relative strength of $|U|$ and $|J|$ (see Ref. 14); assuringly, such features are consistent with the ones observed in borocarbides. In the present context of nonsuperconducting $Tb(Co_xNi_{1-x})_2B_2C$, this model corresponds to $U = 0$ and predicts that a succession of magnetic modes are stabilized as $|J|$ increases. According to the ground state phase diagram of Ref. 14, incommensurate spin-density waves (ISDW's), with a continuously varying k vector, exist for $|J|$ between 0 and some critical value J_{c1}; the SDW becomes commensurate (the AFM equivalent in one dimension, $k = \pi$) for $|J_{c1}| < |J| < |J_{c2}|$, and, finally, a FM state sets in for $|J| > |J_{c2}|$. While the dependence of the effective parameter $|J|$ with Co concentration x cannot be extracted in a straightforward manner, the fact that the model predicts the sequence observed with increasing x can hardly be regarded as fortuitous; the appearance of modes with continuously varying k in Ref. 14, instead of a single $\vec{k}_3$ mode may be attributed to the one-dimensional geometry of the calculations.

This description, nonetheless, needs to be supplemented with other ingredients so as to account for the above-mentioned anomalous behavior of the $x = 0.4$ sample. This indicates that the simple RKKY picture may not be entirely applicable near this concentration, given that the magnitude of the effective local moments is significantly reduced. Other theoretical approaches, such as those of the authors of Refs. 24–26, have been used to describe the effects of an external field in the magnetic phase diagram, but most likely would also need additional ingredients to describe the behavior near $x = 0.4$.

In summary, several experimental techniques have been used to study the evolution of the magnetic properties of $Tb(Co_xNi_{1-x})_2B_2C$. The variation in $M = Co_xNi_{1-x}$ modifies the electron count, and this, in turn, introduces drastic variation in the magnetic structure leading to $\vec{k}$ modes compatible with symmetry requirements: $\vec{k} = (0.55,0,0)$ of the Ni-based end member is transformed, successively, into $\vec{k} = (1/2,0,1/2)$ for $x = 0.2,0.4$, $\vec{k} = (0,0,1/3)$ for $x = 0.6$, and, finally, $\vec{k} = (0,0,0)$ for $x = 0.8,1$. These modifications are accompanied by a lattice adjustment, indicative of strong magnetoelastic forces. Magnetic anomalous behavior was observed in the intermediate $x = 0.4$ concentration. Finally, the confrontation of available theoretical analyses with these results leads us to conclude that the combined effect of electronic structure (i.e., the ensuing competition between FM and AFM effective couplings) with magnetoelastic forces is responsible for shaping both the lattice and magnetic properties of $Tb(Co_xNi_{1-x})_2B_2C$. This scenario can be easily generalized to the wider case of RNi_2B_2C and RCo_2B_2C series.

Partial financial support from the Brazilian Agencies CNPq, CAPES, and FAPERJ is gratefully acknowledged.

[1] B. Coqblin, *The Electronic Structure of Rare-Earth Metals and Aloys: The Magnetic Heavy Rare-Earth* (Academic Press, New York, 1977).
[2] J. Jensen and A. R. Mackintosh, *Rare Earth Magnetism: Structures And Excitations* (Clarendon Press, Oxford, 1991).
[3] R. Nagarajan, C. Mazumdar, Z. Hossain, S. K. Dhar, K. V. Gopalakrishnan, L. C. Gupta, C. Godart, B. D. Padalia, and R. Vijayaraghavan, Phys. Rev. Lett. **72**, 274 (1994).
[4] R. J. Cava, H. Takagi, H. W. Zandbergen, J. J. Krajewski, W. F. Peck Jr., T. Sigerist, B. Batlogg, R. B. V. Dover, R. J. Felder, K. Mizuhashi, J. O. Lee, H. Eisaki, and S. Uchida, Nature (London) **367**, 254 (1994).
[5] K.-H. Müller and V. N. Narozhnyi, Rep. Prog. Phys. **64**, 943 (2001).
[6] P. C. Canfield, P. L. Gammel, and D. J. Bishop, Phys. Today **51**, 40 (1998).
[7] T. Paiva, M. El Massalami, and R. R. dos Santos, J. Phys.: Condens. Matter **15**, 7917 (2003).
[8] L. C. Gupta, Adv. Phys. **55**, 691 (2006).
[9] M. ElMassalami, R. Moreno, H. Takeya, B. Ouladdiaf, J. W. Lynn, and R. S. Freitas, J. Phys.: Condens. Matter **21**, 436006 (2009).
[10] M. ElMassalami, R. Moreno, R. M. Saeed, F. A. B. Chaves, C. M. Chaves, R. E. Rapp, H. Takeya, B. Ouladdiaf, and M. Amara, J. Phys.: Condens. Matter **21**, 216006 (2009).
[11] M. ElMassalami, R. E. Rapp, F. A. B. Chaves, R. Moreno, H. Takeya, B. Ouladdiaf, J. W. Lynn, Q. Huang, R. S. Freitas, and N. F. Oliveria Jr., J. Phys.: Condens. Matter **21**, 046007 (2009).
[12] J. W. Lynn, S. Skanthakumar, Q. Huang, S. K. Sinha, Z. Hossain, L. C. Gupta, R. Nagarajan, and C. Godart, Phys. Rev. B **55**, 6584 (1997).
[13] J. Y. Rhee, X. Wang, and B. N. Harmon, Phys. Rev. B **51**, 15585 (1995).
[14] P. R. Bertussi, A. L. Malvezzi, T. Paiva, and R. R. dos Santos, Phys. Rev. B **79**, 220513 (2009).
[15] L. J. Chang, C. V. Tomy, D. McK. Paul, and C. Ritter, Phys. Rev. B **54**, 9031 (1996).
[16] J. Rodríguez-Carvajal, Physica B **192**, 55 (1993).
[17] T. Siegrist, R. Cava, J. J. Krajewski, and W. F. Peck, J. Alloys Compd. **216**, 135 (1994).
[18] M. ElMassalami, M. Amara, R.-M. Galera, D. Schmitt, and H. Takeya, Phys. Rev. B **76**, 104410 (2007).
[19] H. Kawano-Furukawa, H. Tsukagoshi, T. Nagata, C. Kobayashi, H. Yoshizawa, and H. Takeya, Phys. Rev. B **77**, 144426 (2008).
[20] M. ElMassalami *et al.* (unpublished).
[21] C. Song, Z. Islam, L. Lottermoser, A. I. Goldman, P. C. Canfield, and C. Detlefs, Phys. Rev. B **60**, 6223 (1999).

[22]C. Song, D. Wermeille, A. I. Goldman, P. C. Canfield, J. Y. Rhee, and B. N. Harmon, Phys. Rev. B **63**, 104507 (2001).
[23]A. S. Wills, C. Detlefs, and P. C. Canfield, Philos. Mag. **83**, 1227 (2003).
[24]V. A. Kalatsky and V. L. Pokrovsky, Phys. Rev. B **57**, 5485 (1998).
[25]A. Amici and P. Thalmeier, Phys. Rev. B **57**, 10 684 (1998).
[26]A. Amici, P. Thalmeier, and P. Fulde, Phys. Rev. Lett. **84**, 1800 (2000).